

# Entanglement and magic on the light-front

Sam Alterman\* and Peter J. Love†

Department of Physics and Astronomy, Tufts University, Medford, Massachusetts 02155, USA

(Dated: July 14, 2025)

In the light-front (LF) formulation of quantum field theory (QFT), physics is formulated from the perspective of a massless observer necessarily traveling at the speed of light. The LF formulation provides an alternative computational approach to lattice gauge theory, and has recently been investigated as a future application of quantum computers. A natural question is how quantum resources such as entanglement and contextuality amongst physical qubits in the laboratory are utilized in LF simulations of QFTs. We use the (1+1)D transverse-field Ising model to explore this question. We derive the LF energy operator that generates the LF dynamics of the system, which is distinct from the instant-form (IF) Hamiltonian. We find that while the eigenstates of the IF Hamiltonian exhibit pairwise entanglement between positive and negative momenta in IF momentum-space, the eigenstates of the LF Hamiltonian are separable in LF momentum-space. We then calculate the momentum-space magic of the IF-momentum-space ground state and show that it always requires more magic to prepare than the LF-momentum-space ground state. At the quantum critical point, corresponding to a massless free fermion, both LF and IF ground states are stabilizers, but the LF ground state is separable in LF momentum-space while the IF ground state is a product of maximally entangled pairs in IF momentum-space. These results show that quantum resources such as entanglement and magic are utilized differently by quantum simulations formulated in LF and IF, and that the simplicity of the LF ground state results in fewer required quantum resources.

*Introduction.*— Quantum field theory (QFT) is a natural application for which quantum computing may perform simulations beyond the capabilities of classical computers [1–5]. Recently, the question of how quantum resources such as entanglement, contextuality and magic can be most efficiently utilized in quantum simulations of QFT has attracted much attention [6–11]. Most approaches to quantum simulations of QFT use the instant form (IF) representation of QFTs in which all observables lie on a spacelike hypersurface. IF coordinates  $x^0$  and  $x^1$  describe Minkowskian spacetime as seen by a massive observer in an inertial reference frame with the (1+1)D metric  $g_{00} = -g_{11} = 1$ ,  $g_{10} = g_{01} = 0$ . However, Dirac [12] showed that the IF is not the only valid formulation of relativistic quantum mechanics. Light-front (LF) coordinates describe the perspective of a massless observer. LF coordinates in (1+1)D are defined as  $x^\pm = x^0 \pm x^1$ , with  $x^+$  playing the role of light-front “time” and  $x^-$  playing the role of light-front “space”. The metric is  $g^{+-} = g^{-+} = 2$ ,  $g^{++} = g^{--} = 0$  [12–14]. It was first realized by Wilson [15] that the LF formulation results in representations of QFTs that show a remarkable similarity to well-studied problems in quantum chemistry, and LF simulations of QFTs have recently been investigated as an approach for efficiently simulating quantum field theory on a quantum computer [16–23].

A natural question is how quantum resources change between the IF and LF representations of a QFT. In this work, we consider entanglement, contextuality and magic as resources for quantum computing [24–26]. Suppose we have a quantum computer which we wish to use to simulate a QFT. Assuming the quantum computer is made of massive components its quantum resources will

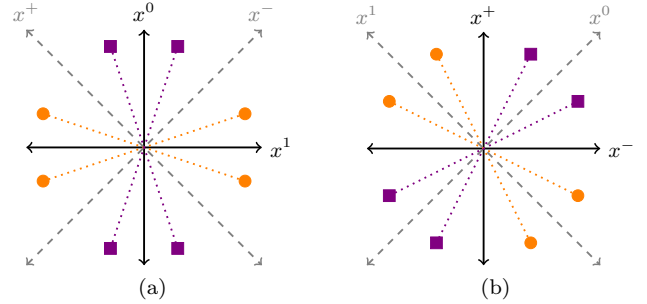


FIG. 1. (a) Spacetime diagram showing Bell type measurements testing entanglement (orange circles) and Kochen-Specker type measurements testing contextuality (purple squares) in instant-time coordinates. (b) The same measurements as viewed in light-front coordinates. A quantum computer where LF space and time in the simulation correspond to IF space and time in the lab would have Bell type measurements in the lab which correspond to Kochen-Specker type measurements in the theory, and vice versa.

be defined in the (IF) inertial laboratory frame. Mermin [27] notes that entanglement can be conceptualized as emerging when non-contextuality is required by locality. Through this framework, Bell tests of entanglement can be associated with spacelike separations while Kochen-Specker tests of contextuality can be associated with timelike measurements, as depicted in Fig. 1a [28, 29]. This perspective allows us to see that if we set up our simulation such that (IF) physical space and time in the laboratory frame correspond to LF space and time respectively in the simulation, the relationship between quantum resources in the QFT and quantum resources

on the physical device is non-trivial. As seen in Fig. 1b, the structure of LF coordinates means that (space-like) entanglement between two qubits in the lab frame could correspond to either entanglement or contextuality in the QFT, and entanglement in the QFT could correspond to either (spacelike) entanglement or (timelike) contextuality in the lab frame. Because the utilization of quantum resources in QFTs is an active area of research, we are motivated to study how resources change on the LF through a toy model which is well understood but still allows us to utilize the LF framework.

The TFIM is a well studied system that exhibits fermionic behavior in the vicinity of  $\lambda = 1$  [30–34]. This is the critical point of a quantum phase transition between ferromagnetic and antiferromagnetic behavior, with an associated diverging correlation length  $\xi \sim a|1 - \lambda|^{-1}$  [30, 35]. In this work, we consider a transverse field Ising model (TFIM) consisting of a linear chain of  $N$  spins with spacing  $a$  and physical length  $L = Na$  oriented along the  $x$  axis. We assume  $N$  to be even. Each spin is coupled to nearest neighbors and subjected to a transverse magnetic field of relative strength  $\lambda$  along the  $z$  axis, resulting in a Hamiltonian for the system given (in IF coordinates) by

$$H_{IF} = -\frac{1}{2} \sum_j X_j X_{j+1} - \frac{\lambda}{2} \sum_j Z_j \quad (1)$$

where  $X_j$  ( $Z_j$ ) is a Pauli matrix applied to the  $j^{\text{th}}$  spin in the chain. We will assume  $N$  to be even and sufficiently large as to neglect boundary terms. Using the Jordan-Wigner transformation [36] to define fermionic operators

$$c_j = \frac{X_j - iY_j}{2} \prod_{j' < j} Z_{j'}, \quad (2)$$

the Hamiltonian (1) is expressed in fermionic form as

$$H_{IF} = \sum_j \left[ \frac{\lambda}{2} (2c_j^\dagger c_j - 1) - \frac{1}{2} (c_j^\dagger - c_j) (c_{j+1}^\dagger + c_{j+1}) \right] \quad (3)$$

where we have assumed the fermionic spatial periodic boundary condition  $c_{N+1} = c_1$  [37]. Assuming  $N$  to be sufficiently large as to approximate the momentum  $k$  as continuous over  $(-\pi/a, \pi/a]$ , the Hamiltonian (3) can be written in momentum space as [32–34]

$$H = \int_0^{\pi/a} dk \, 2\omega_k \left( \hat{\gamma}_k^\dagger \hat{\gamma}_k + \hat{\gamma}_{-k}^\dagger \hat{\gamma}_{-k} - 1 \right) \quad (4)$$

$$\omega_k = \sqrt{\lambda^2 - 2\lambda \cos(ka) + 1}$$

with  $\hat{O}_k$  denoting that an operator  $O$  acts in momentum space and  $\hat{\gamma}_k = \cos \theta_k \hat{c}_k + i \sin \theta_k \hat{c}_{-k}^\dagger$ ,  $\tan 2\theta_k = \frac{\sin(ka)}{\lambda - \cos(ka)}$ .

A thorough derivation of (4) is given in the Appendix. We can then see that for  $ka \ll 1$ ,  $\lambda \approx 1$ , the spectrum becomes the relativistic dispersion relation of a free fermion  $\omega_k = \sqrt{m^2 + k^2}$  with mass  $m = (1 - \lambda)/a$ . In the vicinity of the quantum critical point  $\lambda = 1$ , the mass will be determined by how we take the limits  $\lambda \rightarrow 1$  and  $a \rightarrow 0$ .

To map the system onto a fermionic field, we define at each point on the chain in IF space  $x_j = aj$  a field spinor  $\Psi(x_j) = \begin{pmatrix} c_j \\ c_j^\dagger \end{pmatrix}$ . Taking the continuum limit  $a \rightarrow 0$ , when  $\lambda \rightarrow 1$  (and thus  $\xi \gg a$ ) the IF dynamics of  $\Psi$  are modeled by the free fermion Dirac equation [38]

$$(i\gamma^0 \partial_0 + i\gamma^1 \partial_1 - m)\Psi = 0 \quad (5)$$

with  $x^0 = at$ ,  $x^1 = ja$ , mass  $m = (1 - \lambda)/a$ , and gamma matrices  $\gamma^0 = Z$  and  $\gamma^1 = iX$  [39].

*The TFIM on the light-front.*— We now consider the TFIM on the LF. The evolution is governed by the Dirac equation, written in terms of LF derivatives as

$$(i\gamma^+ \partial_+ + i\gamma^- \partial_- - m)\Psi = 0 \quad (6)$$

with gamma matrices  $\gamma^+ = \gamma^0 + \gamma^1 = Z + iX$  and  $\gamma^- = \gamma^0 - \gamma^1 = Z - iX$ . We follow [40] and define orthogonal projectors  $\Lambda^{(\pm)} = \frac{1}{4} \gamma^\mp \gamma^\pm = \frac{1}{2} (1 \mp Y)$ . These projectors allow us to split  $\Psi$  into two components  $\Psi^{(+)}$  and  $\Psi^{(-)}$  given by

$$\Psi^{(\pm)} = \Lambda^{(\pm)} \Psi = \frac{1}{\sqrt{2}} \begin{pmatrix} 1 \\ \mp i \end{pmatrix} \psi_\pm, \quad \psi_\pm = \frac{1}{\sqrt{2}} (c \pm ic^\dagger). \quad (7)$$

From (6), we obtain one dynamical equation

$$2i\partial_+ \Psi^{(+)} = m\gamma^0 \Psi^{(-)} \quad (8a)$$

which gives the variation of  $\Psi^{(+)}$  (termed the “good” fermion) with LF time  $x^+$  and one kinematical equation

$$2i\partial_- \Psi^{(-)} = m\gamma^0 \Psi^{(+)} \quad (8b)$$

which gives the variation of  $\Psi^{(-)}$  (termed the “bad” fermion) with LF space  $x^-$  [13, 40].

The equations of motion for  $m \neq 0$  (8) are associated with the LF action

$$\mathcal{S} = \int dx^+ dx^- \bar{\Psi} (i\gamma^+ \partial_+ + i\gamma^- \partial_- - m) \Psi. \quad (9)$$

from which we obtain the LF energy operator [13, 40]

$$P^- = \frac{m}{2} \int_{-\infty}^{\infty} dx^- \psi_+^\dagger \psi_-. \quad (10)$$

We will discuss the  $m = 0$  case separately below.

*Momentum-space eigenstates and quantum resources.*— To quantize neutral fermionic fields in momentum space, we utilize the approach of discretized light cone quantization (DLCQ) [13]. In IF

coordinates, the time evolution is governed by the IF energy operator  $P^0$ , which we quantize in a periodic box  $x^1 \in [-\frac{L}{2}, \frac{L}{2}]$  with IF momentum and IF energy given by

$$k_n^1 = \frac{2\pi n}{L}, \quad n = -\frac{N}{2}, -\frac{N}{2} + 1, \dots, \frac{N}{2} - 1; \quad (11)$$

$$(k_n^0)^2 - (k_n^1)^2 = m^2.$$

In the limit  $L \rightarrow \infty$ , the momenta  $k_n^1$  densely fill the interval  $(-\pi/a, \pi/a]$  and can be approximated as continuous. Applying the Fourier transform

$$c = \int_{-\pi/a}^{\pi/a} \frac{dk^1}{\sqrt{2\pi}} \hat{c}_k e^{-ik^1 x^1} = \int_{-\pi/a}^{\pi/a} \frac{dk^1}{\sqrt{2\pi}} \hat{c}_k e^{-i(k^0 x^0 + k^1 x^1)}, \quad (12)$$

the momentum-space form of the IF energy operator is written in diagonal form as

$$H_{IF} = \int_0^\infty dk \, 2\omega_k \left( \hat{\eta}_k^\dagger \hat{\eta}_k + \hat{\eta}_{-k}^\dagger \hat{\eta}_{-k} - 1 \right) \quad (13)$$

$$\omega_k = \sqrt{m^2 + k^2}$$

with  $\hat{\eta}_k = \cos \phi_k \hat{c}_k + i \sin \phi_k \hat{c}_{-k}^\dagger$ ,  $\tan(2\phi_k) = k/m$ , which is a small  $ka$  approximation of the Bogoliubov transformation in (4), consistent with the  $a \rightarrow 0$  continuum limit.

The IF Hamiltonian (13) is block diagonal with blocks labelled by absolute momentum  $|k|$ . The ground state of each block is:

$$|\Phi_k\rangle = \left( \cos \phi_k - i \sin \phi_k \hat{c}_k^\dagger \hat{c}_{-k}^\dagger \right) |0\rangle_k |0\rangle_{-k} \quad (14)$$

where  $|0\rangle_k$  is the fermionic vacuum state of  $\hat{c}_k^\dagger \hat{c}_k$ . The overall ground state  $|\Phi\rangle = \otimes_{k>0} |\Phi_k\rangle$  is the BCS-type ground state

$$|\Phi\rangle = \bigotimes_{k>0} \left( \cos \phi_k |0\rangle_k |0\rangle_{-k} - i \sin \phi_k |1\rangle_k |1\rangle_{-k} \right) \quad (15)$$

and excited states are:

$$|k'\rangle = \hat{\eta}_{k'}^\dagger |\Phi\rangle = |1\rangle_k |0\rangle_{-k'} \bigotimes_{\substack{k>0 \\ k \neq k'}} |\Phi_k\rangle \quad (16)$$

with energies  $E_k = 2\sqrt{m^2 + k^2}$  [32–34].

We will now consider LF momentum-space representation of the LF energy operator (10). Quantizing in a box  $x^- \in [-\frac{L}{2}, \frac{L}{2}]$  with a periodic boundary condition [41], the LF momentum  $k^+$  and LF energy  $k^-$  are given by [13]

$$k_n^+ a = \frac{2\pi n}{N}, \quad n = 1, 2, \dots, N; \quad k_n^+ k_n^- = m^2 \quad (17)$$

Again assuming  $L \rightarrow \infty$ , the LF Fourier transform is

$$\psi_+ = \int_0^{2\pi/a} \frac{dk^+}{\sqrt{2\pi}} \tilde{c}_{k^+} e^{-i(k^+ x^- + k^- x^+)/2}, \quad (18)$$

and we derive from (8)

$$\psi_- = \int_0^{2\pi/a} \frac{dk^+}{\sqrt{2\pi}} \frac{m}{k^+} \tilde{c}_{k^+} e^{-i(k^+ x^- + k^- x^+)/2}, \quad (19)$$

where  $\tilde{c}$  denotes that the operator is acting in LF momentum space.

Substituting in to the LF energy operator (10) and setting  $x^+ = 0$ , we then find the momentum space LF Hamiltonian

$$H_{LF} = \int_0^\infty dk^+ \frac{m^2}{2k^+} \tilde{c}_{k^+}^\dagger \tilde{c}_{k^+}. \quad (20)$$

Hence (20) is diagonalized in LF momentum space. The eigenstates of the LF momentum-space Hamiltonian (20) are:

$$|k^+\rangle = \tilde{c}_{k^+}^\dagger |0\rangle_{k^+} \quad (21)$$

with energies  $E_{k^+} = m^2/(2k^+)$ . The form of (14) shows that while the IF eigenstates exhibit entanglement between momentum  $+k$  and momentum  $-k$ , the LF eigenstates (21) are entirely separable in both LF and IF momentum-space.

In addition to entanglement, another resource for quantum computing is the non-stabilizerness or “magic”, which is associated with the level of non-stabilizerness or contextuality [24, 42–48]. To quantify the non-stabilizerness of the IF and LF eigenstates, we utilize the framework of stabilizer Rényi entropy (SRE) [49–52]. To evaluate resources in momentum-space, we follow [52] and define momentum-space qubits through the inverse Jordan-Wigner transformation [53]

$$\frac{1}{2} (\hat{X}_k + i\hat{Y}_k) = \hat{c}_k^\dagger \exp \left( i\pi \sum_{k' < k} \hat{c}_{k'}^\dagger \hat{c}_{k'} \right) \quad (22)$$

$$\hat{Z}_k = 2\hat{c}_k^\dagger \hat{c}_k - 1.$$

The SRE of the ground state  $|\Phi\rangle$  is then defined as [49]

$$M_q \equiv \frac{1}{1-q} \ln \left( \frac{1}{4^N} \sum_{P \in P^{(N)}} |\langle \Phi | P | \Phi \rangle|^{2q} \right) \quad (23)$$

where  $P^{(N)} = \{I, X, Y, Z\}^{\otimes N}$  is the set of all  $4^N$  possible momentum-space Pauli strings.

Because the LF ground state is separable in LF-momentum-space, it is a stabilizer state with  $M_2^{LF} = 0$ . The IF ground state (15) factorizes by absolute momentum. Taking  $|0\rangle_k$  to be the  $-1$  eigenstate of  $\hat{Z}_k$  and  $|1\rangle_k$  to be the  $+1$  eigenstate, the non-zero ground state expectation values in each of the  $N/2$  4-dimensional subspaces are then

$$\begin{aligned} \langle \Phi_k | \hat{I}_k \hat{I}_{-k} | \Phi_k \rangle &= \langle \Phi_k | \hat{Z}_k \hat{Z}_{-k} | \Phi_k \rangle = 1 \\ \langle \Phi_k | \hat{I}_k \hat{Z}_{-k} | \Phi_k \rangle &= \langle \Phi_k | \hat{Z}_k \hat{I}_{-k} | \Phi_k \rangle = -\cos(2\phi_k) \\ \langle \Phi_k | \hat{X}_k \hat{Y}_{-k} | \Phi_k \rangle &= \langle \Phi_k | \hat{Y}_k \hat{X}_{-k} | \Phi_k \rangle = \sin(2\phi_k), \end{aligned} \quad (24)$$

with the other 10 expectation values being zero [52]. The “magic”  $M_2$  is then

$$M_2^{IF} = -\ln \left( \prod_{k>0} \frac{1 + \cos^4(2\phi_k) + \sin^4(2\phi_k)}{2} \right) \quad (25)$$

$$= -\sum_{k>0} \ln \left( 1 - \left( \frac{km}{k^2 + m^2} \right)^2 \right).$$

Because for  $m > 0$ , the  $m = k$  term (corresponding to  $\phi_k = \pi/4$ ) will always contribute  $\ln(4/3) \approx 0.288$ , we can see that for all  $m > 0$  the IF ground state will require more magic to prepare than the LF ground state.

*The phase transition.*— We will now consider the behavior at the quantum critical point  $\lambda = 1$ , corresponding to a massless free fermion in the field representation. The IF Hamiltonian (13) remains well behaved at  $\lambda = 1$ , leaving us with

$$H_{\text{IF}}^{(m=0)} = \int_0^\infty dk \, 2k \left( \hat{\eta}_k^\dagger \hat{\eta}_k + \hat{\eta}_{-k}^\dagger \hat{\eta}_{-k} - 1 \right) \quad (26)$$

where now  $\hat{\eta}_k = \frac{1}{\sqrt{2}}(\hat{c}_k - i\hat{c}_{-k}^\dagger)$ . The ground state then becomes the maximally entangled Bell state

$$|\Phi\rangle = \bigotimes_{k>0} \left( \frac{1}{\sqrt{2}} |0\rangle_k |0\rangle_{-k} - \frac{i}{\sqrt{2}} |1\rangle_k |1\rangle_{-k} \right). \quad (27)$$

Because each  $|\Phi_k\rangle$  in (27) is now a stabilizer in the momentum-space qubitization (22), the IF magic (25) now goes to zero.

A consequence of (8) is that in the massless case, the “good” fermion  $\Psi^{(+)}$  becomes LF time-invariant and the “bad” fermion  $\Psi^{(-)}$  becomes LF space-invariant, requiring particular care when quantizing these variables. For our purposes, we follow the approach of [54] and quantize  $P^-$  independently of  $k^+$  in the massless case to allow for a direct comparison with the IF energy operator  $P^0$ ; however, we note that the proper LF quantization of massless fields and the connection to zero modes remains an area of active research [55, 56]. From the LF dispersion relation (17), we can see that  $k^+$  in the  $m = 0$  case will no longer be a good variable with which to quantize the LF energy operator  $P^-$  as  $k^- = 0$  for any  $k^+ > 0$  [55, 56]. This leads us, following the approach of [54], to instead quantize in terms of  $k^-$ , resulting in a form of (20) as

$$H_{LF} = \frac{1}{2} \int_0^\infty dk^- \, k^- \hat{c}_{k^-}^\dagger \hat{c}_{k^-} \quad (28)$$

We then note that when  $m = 0$ , (11) implies  $k^0 = |k^1|$ , resulting in two potential cases for our LF quantized energy and momenta:

$$\begin{aligned} k^1 > 0: \quad & k^+ = 2k^1, \, k^- = 0 \\ k^1 < 0: \quad & k^+ = 0, \, k^- = -2k^1. \end{aligned} \quad (29)$$

This leads us to then write

$$H_{LF}^{(m=0)} = \int_0^\infty dk \, 2k \, \hat{c}_{-2k}^\dagger \hat{c}_{-2k}, \quad (30)$$

which is equivalent to the diagonalized massless IF Hamiltonian (26) with only negative even momenta included, and the massless LF eigenstates will thus be of the form

$$|k^-\rangle = \hat{c}_{-2k}^\dagger |0\rangle. \quad (31)$$

Thus, even while LF and IF quantization coincide at the quantum critical point, the LF ground state (31) remains distinct from the IF ground state (27), and remains entirely separable in momentum-space while the IF ground state is maximally entangled.

*Discussion.*— In this paper, we used the transverse field Ising model (TFIM) to explore quantum resources in IF and LF coordinates. We derived the Hamiltonians in both LF and IF momentum space, and show that the LF Hamiltonian is diagonal without the Bogoliubov transformation required in IF. The eigenstates of the LF Hamiltonian are separable in LF momentum space, while the eigenstates of the IF Hamiltonian have pairwise entanglement between modes with momentum  $\pm k$  in IF momentum space. We quantified the non-stabilizerness, or magic, of the ground states using momentum-space stabilizer Rènyi entropy. At the quantum critical point  $\lambda = 1$  (corresponding to a massless free fermion) the IF states are also stabilizer states, though still exhibiting entanglement between positive and negative momenta.

The simplicity of the LF ground state has been known for some time and is an active area of research [57–61], we see it emerge here simply from the form of LF quantization. The entanglement exhibited by IF ground states emerges from the Kramers-Wannier duality between a particle with momentum  $+k$  and a hole with momentum  $-k$ , which results in a block-diagonal structure in momentum-space. But the form of the LF Hamiltonian  $P^- = P^0 - P^1$  does not permit such a coupling, breaking the duality and resulting in a LF Hamiltonian which is diagonal in LF momentum without the need for a Bogoliubov transformation. While the LF has been actively studied for high energy and nuclear physics for more than 75 years, this work represents the first discussion of quantum resources on the light front. Extension of the current study to interacting theories, higher dimensions, and consideration of the effects of renormalization are all promising future directions.

We wish to thank Kamil Serafin, Carter Gustin, Michael Kreschuk, Feng Qian, James Vary, and Natalie Klco for useful advice and discussion. This work was supported by the United States Department of Energy under the Office of Science Quantum Information Science Research Centers for the Quantum Systems Accelerator (QSA) program (7568717) and under the

Office of Nuclear Physics Quantum Horizons program for the **Nuclei** and **Hadrons with Quantum Computers** (NuHaQ) project (DE-SC0023707).

*Appendix.*— In this appendix, we more thoroughly derive the diagonalization of the transverse-field Ising model Hamiltonian (3) in (IF) momentum space. To work in momentum-space, we utilize the Fourier transforms

$$\hat{c}_k = \frac{1}{\sqrt{N}} \sum_{j=1}^N e^{-ikja} c_j, \quad \hat{c}_k^\dagger = \frac{1}{\sqrt{N}} \sum_{j=1}^N e^{ikja} c_j^\dagger. \quad (\text{A.1})$$

To understand which values of momentum to use, we note that our fermionic boundary condition requires  $c_N = c_1$  and thus  $\sum_k e^{ik(N+1)a} = \sum_k e^{ika}$  or  $e^{ikNa} = 1$  for all  $k$ . Thus, the  $N$  allowable values of  $k$  are

$$k \in \left\{ \frac{2\pi n}{L}, \quad n = -\frac{N}{2}, -\frac{N}{2} + 1, \dots, \frac{N}{2} - 1 \right\}. \quad (\text{A.2})$$

For  $L \rightarrow \infty$ , we can see that the spacing between the allowable momenta vanishes, allowing us to treat the momentum as continuous over  $[-\pi/a, \pi/a]$ .

We then utilize the identity

$$\lim_{N \rightarrow \infty} \sum_{j=1}^N e^{2\pi i j(n-m)/N} = \delta_{n,m}, \quad (\text{A.3})$$

which allows us to write the Hamiltonian (3) in momentum space as

$$\begin{aligned} H_{IF} &= \sum_k \left[ 2(\lambda - \cos(ka)) \hat{c}_k^\dagger \hat{c}_k - (\lambda - e^{-ika}) \right. \\ &\quad \left. - e^{ika} (\hat{c}_k^\dagger \hat{c}_{-k}^\dagger + \hat{c}_k \hat{c}_{-k}) \right] \\ &= \sum_{k>0} \left[ 2(\lambda - \cos(ka)) (\hat{c}_k^\dagger \hat{c}_k + \hat{c}_{-k}^\dagger \hat{c}_{-k} - 1) \right. \\ &\quad \left. - 2i \sin(ka) (\hat{c}_k^\dagger \hat{c}_{-k}^\dagger + \hat{c}_k \hat{c}_{-k}) \right]. \end{aligned} \quad (\text{A.4})$$

We observe that the momentum-space Hamiltonian (A.4) is block-diagonal in momentum space, with each block  $H_k$  corresponding to a single absolute momentum  $k$ . Each block is made up of four terms: a number operator  $\hat{c}_k^\dagger \hat{c}_k$  for particles with momentum  $+k$ ; a number operator  $\hat{c}_{-k}^\dagger \hat{c}_{-k}$  for particles with momentum  $-k$ ; a creation operator  $\hat{c}_k^\dagger \hat{c}_{-k}^\dagger$  which creates a pair of particles, one with momentum  $+k$  and one with momentum  $-k$ ; and the corresponding annihilation operator  $\hat{c}_k \hat{c}_{-k}$ .

To diagonalize the blocks, we introduce the Bogoliubov transformation

$$\hat{\gamma}_k = \cos \theta_k \hat{c}_k + i \sin \theta_k \hat{c}_{-k}^\dagger. \quad (\text{A.5})$$

Substituting in to (A.4), we find

$$\begin{aligned} H_k &= 2((\lambda - \cos(ka)) \cos 2\theta_k + \sin(ka) \sin 2\theta_k) (\hat{\gamma}_k^\dagger \hat{\gamma}_k + \hat{\gamma}_{-k}^\dagger \hat{\gamma}_{-k} - 1) \\ &\quad + 2i(-(\lambda - \cos(ka)) \sin 2\theta_k + \sin(ka) \cos 2\theta_k) (\hat{\gamma}_k^\dagger \hat{\gamma}_{-k}^\dagger + \hat{\gamma}_k \hat{\gamma}_{-k}). \end{aligned} \quad (\text{A.6})$$

We can thus see that  $H_k$  will be diagonalized when

$$-(\lambda - \cos(ka)) \sin 2\theta_k + \sin(ka) \cos 2\theta_k = 0, \quad (\text{A.7})$$

giving us the constraint equation for  $\theta_k$

$$\tan 2\theta_k = \frac{\sin(ka)}{\lambda - \cos(ka)}. \quad (\text{A.8})$$

We can then write

$$\begin{aligned} \cos 2\theta_k &= \frac{\lambda - \cos(ka)}{\sqrt{\lambda^2 - 2\lambda \cos(ka) + 1}}, \\ \sin 2\theta_k &= \frac{\sin(ka)}{\sqrt{\lambda^2 - 2\lambda \cos(ka) + 1}} \end{aligned} \quad (\text{A.9})$$

and thus

$$(\lambda - \cos(ka)) \cos 2\theta_k + \sin(ka) \sin 2\theta_k = \sqrt{\lambda^2 - 2\lambda \cos(ka) + 1} \equiv \omega_k. \quad (\text{A.10})$$

We then arrive at

$$H_{IF} = \sum_k 2\omega_k (\hat{\gamma}_k^\dagger \hat{\gamma}_k + \hat{\gamma}_{-k}^\dagger \hat{\gamma}_{-k} - 1). \quad (\text{A.11})$$

\* sam.alterman@tufts.edu

† peter.love@tufts.edu

- [1] C. W. Bauer, Z. Davoudi, A. B. Balantekin, T. Bhattacharya, M. Carena, W. A. d. Jong, P. Draper, A. El-Khadra, N. Gemelke, M. Hanada, D. Kharzeev, H. Lamm, Y.-Y. Li, J. Liu, M. Lukin, Y. Meurice, C. Monroe, B. Nachman, G. Pagano, J. Preskill, E. Rinaldi, A. Roggero, D. I. Santiago, M. J. Savage, I. Siddiqi, G. Siopsis, D. V. Zanten, N. Wiebe, Y. Yamauchi, K. Yeter-Aydeniz, and S. Zorsetti, Quantum simulation for high-energy physics, *PRX Quantum* **4**, 027001 (2023).
- [2] C. W. Bauer, Z. Davoudi, N. Klco, and M. J. Savage, Quantum simulation of fundamental particles and forces, *Nat. Rev. Phys.* **5**, 420 (2023).
- [3] S. P. Jordan, K. S. M. Lee, and J. Preskill, Quantum algorithms for quantum field theories, *Science* **336**, 1130 (2012).
- [4] S. P. Jordan, K. S. M. Lee, and J. Preskill, Quantum algorithms for fermionic quantum field theories, arXiv:1404.7115.
- [5] S. P. Jordan, H. Krovi, K. S. M. Lee, and J. Preskill, BQP-completeness of scattering in scalar quantum field theory, *Quantum* **2**, 44 (2018).
- [6] N. Klco, A. Roggero, and M. J. Savage, Standard model physics and the digital quantum revolution: thoughts about the interface, *Rep. Prog. Phys.* **85**, 064301 (2022).
- [7] P. Calabrese and J. Cardy, Entanglement entropy and quantum field theory, *J. Stat. Mech.* **2004**, P06002 (2004).
- [8] P. V. Buividovich and M. I. Polikarpov, Entanglement entropy in lattice gauge theories, *J. Phys. A* **42**, 304005 (2009).
- [9] H. Casini, M. Huerta, and J. A. Rosabal, Remarks on entanglement entropy for gauge fields, *Phys. Rev. D* **89**, 085012 (2014).
- [10] N. Klco, D. H. Beck, and M. J. Savage, Entanglement structures in quantum field theories: Negativity cores and bound entanglement in the vacuum, *Phys. Rev. A* **107**, 012415 (2023).
- [11] N. Klco and D. H. Beck, Entanglement structures in quantum field theories. II. Distortions of vacuum correlations through the lens of local observers, *Phys. Rev. A* **108**, 012429 (2023).
- [12] P. A. M. Dirac, Forms of relativistic dynamics, *Rev. Mod. Phys.* **21**, 392 (1949).
- [13] H.-C. Pauli and S. J. Brodsky, Solving field theory in one space and one time dimension, *Phys. Rev. D* **32**, 1993 (1985).
- [14] H.-C. Pauli and S. J. Brodsky, Discretized light-cone quantization: Solution to a field theory in one space and one time dimension, *Phys. Rev. D* **32**, 2001 (1985).
- [15] K. G. Wilson, Ab initio quantum chemistry: A source of ideas for lattice gauge theorists, *Nucl. Phys. B - Proc. Suppl.* **17**, 82 (1990).
- [16] M. Kreshchuk, S. Jia, W. M. Kirby, G. Goldstein, J. P. Vary, and P. J. Love, Simulating hadronic physics on noisy intermediate-scale quantum devices using basis light-front quantization, *Phys. Rev. A* **103**, 062601 (2021).
- [17] M. Kreshchuk, S. Jia, W. M. Kirby, G. Goldstein, J. P. Vary, and P. J. Love, Light-front field theory on current quantum computers, *Entropy* **23**, 597 (2021).
- [18] M. Kreshchuk, W. M. Kirby, G. Goldstein, H. Beauchemin, and P. J. Love, Quantum simulation of quantum field theory in the light-front formulation, *Phys. Rev. A* **105**, 032418 (2022).
- [19] M. Kreshchuk, J. P. Vary, and P. J. Love, Simulating scattering of composite particles, arXiv:2310.13742.
- [20] C. M. Gustin and G. Goldstein, Generalized parton distribution functions via quantum simulation of quantum field theory in light-front coordinates, arXiv:2211.07826.
- [21] S. Wu, W. Du, X. Zhao, and J. P. Vary, Efficient and precise quantum simulation of ultrarelativistic quark-nucleus scattering, *Phys. Rev. D* **110**, 056044 (2024).
- [22] W. Qian, M. Li, C. A. Salgado, and M. Kreshchuk, Efficient quantum simulation of QCD jets on the light front, arXiv:2411.09762.
- [23] W. A. Simon, C. M. Gustin, K. Serafin, A. Ralli, G. R. Goldstein, and P. J. Love, Ladder operator block-encoding, arXiv:2503.11641.
- [24] R. W. Spekkens, Negativity and contextuality are equivalent notions of nonclassicality, *Phys. Rev. Lett.* **101**, 020401 (2008).
- [25] M. Howard, J. Wallman, V. Veitch, and J. Emerson, Contextuality supplies the ‘magic’ for quantum computation, *Nature* **510**, 351 (2014).
- [26] J. Bermejo-Vega, N. Delfosse, D. E. Browne, C. Okay, and R. Raussendorf, Contextuality as a resource for models of quantum computation with qubits, *Phys. Rev. Lett.* **119**, 120505 (2017).
- [27] N. D. Mermin, Hidden variables and the two theorems of John Bell, *Rev. Mod. Phys.* **65**, 803 (1993).
- [28] J. S. Bell, On the Einstein Podolsky Rosen paradox, *Physics* **1**, 195 (1964).
- [29] S. Kochen and E. Specker, The problem of hidden variables in quantum mechanics, *J. Math. Mech.* **17**, 59 (1967).
- [30] A. Dutta, G. Aeppli, B. K. Chakrabarti, U. Divakaran, T. F. Rosenbaum, and D. Sen, *Quantum Phase Transitions in Transverse Field Spin Models: From Statistical Physics to Quantum Information* (Cambridge University Press, 2015).
- [31] G. Tóth, Entanglement witnesses in spin models, *Phys. Rev. A* **71**, 010301 (2005).
- [32] G. B. Mbeng, A. Russomanno, and G. E. Santoro, The quantum Ising chain for beginners, arXiv:2009.09208.
- [33] G. Mussardo, *Statistical Field Theory: An Introduction to Exactly Solved Models in Statistical Physics*, 2nd ed., Oxford Graduate Texts (Oxford University Press, 2020).
- [34] E. Fradkin, *Quantum Field Theory: An Integrated Approach* (Princeton University Press, 2021).
- [35] E. Lieb, T. Schultz, and D. Mattis, Two soluble models of an antiferromagnetic chain, *Ann. Phys.* **16**, 407 (1961).
- [36] P. Jordan and E. Wigner, Über das Paulische Äquivalenzverbot, *Z. Phys.* **47**, 631 (1928).
- [37] We note that this fermionic boundary condition is distinct from the spin periodic boundary condition  $X_N = X_1$ , which splits the Hamiltonian into two orthogonal spaces based on fermion number parity [32]. However, because we will be taking the large  $N$  limit and treating the spectrum as continuous, this nuance can be safely neglected.
- [38] R. A. Ferrell, Field theory of the two-dimensional Ising model: Equivalence to the free particle one-dimensional Dirac equation, *J. Stat. Phys.* **8**, 265 (1973).
- [39] We note that the gamma matrices do not act on the spins themselves but instead on the spinor  $\Psi(x)$ , and thus the Pauli matrices used to define the gamma matrices have an entirely distinct physical meaning from the Pauli

- matrices used to define the IF Hamiltonian (1).
- [40] P. D. Mannheim, Equivalence of light-front quantization and instant-time quantization, *Phys. Rev. D* **102**, 025020 (2020).
  - [41] We note that the IF and LF boundary conditions are distinct and thus a particular value of  $k_n^+$  does not necessarily translate to an allowed value of  $k_n^1$ . However, because we are assuming the thermodynamic limit  $N \rightarrow \infty$  and treating  $k^1$  and  $k^+$  as continuous, we can safely neglect this nuance.
  - [42] S. Bravyi and A. Kitaev, Universal quantum computation with ideal Clifford gates and noisy ancillas, *Phys. Rev. A* **71**, 022316 (2005).
  - [43] D. Gottesman and I. L. Chuang, Demonstrating the viability of universal quantum computation using teleportation and single-qubit operations, *Nature* **402**, 390 (1999).
  - [44] V. Veitch, S. A. H. Mousavian, D. Gottesman, and J. Emerson, The resource theory of stabilizer quantum computation, *New J. Phys.* **16**, 013009 (2014).
  - [45] S. Bravyi, G. Smith, and J. A. Smolin, Trading classical and quantum computational resources, *Phys. Rev. X* **6**, 021043 (2016).
  - [46] E. Chitambar and G. Gour, Quantum resource theories, *Rev. Mod. Phys.* **91**, 025001 (2019).
  - [47] Z.-W. Liu and A. Winter, Many-body quantum magic, *PRX Quantum* **3**, 020333 (2022).
  - [48] M. Beverland, E. Campbell, M. Howard, and V. Kliuchnikov, Lower bounds on the non-Clifford resources for quantum computations, *Quantum Sci. Technol.* **5**, 035009 (2020).
  - [49] L. Leone, S. F. Oliviero, and A. Hamma, Stabilizer Rényi entropy, *Phys. Rev. Lett.* **128**, 050402 (2022).
  - [50] T. Haug and L. Piroli, Stabilizer entropies and nonstabilizerness monotones, *Quantum* **7**, 1092 (2023).
  - [51] X. Turkeshi, A. Dymarsky, and P. Sierant, Pauli spectrum and nonstabilizerness of typical quantum many-body states, *Phys. Rev. B* **111**, 054301 (2025).
  - [52] B. Dóra and C. P. Moca, Momentum space magic for the transverse field quantum Ising model, arXiv:2412.13560.
  - [53] To construct the Jordan-Wigner string operator  $\exp\left(i\pi \sum_{k' < k} \hat{c}_k^\dagger \hat{c}_{k'}\right)$  in IF momentum-space, we again follow [52] and order the IF momenta in a sequence of opposite pairs  $-k_1, k_1, -k_2, k_2, -k_3, k_3, \dots$  where  $k_i > 0$  but the adjacent pairs need not have any particular order.
  - [54] K. J. Hornbostel, *The application of light-cone quantization to quantum chromodynamics in one-plus-one dimensions*, Ph.D. thesis, Stanford Linear Accelerator Center, Stanford, California (1988).
  - [55] L. Martinović and P. Grangé, Solvable models with massless light-front fermions, *Few-Body Syst.* **56**, 607 (2015).
  - [56] L. Martinović and P. Grangé, Two-Dimensional Massless Light Front Fields and Solvable Models, *Few-Body Syst.* **57**, 565 (2016).
  - [57] P. D. Mannheim, P. Lowdon, and S. J. Brodsky, Structure of light-front vacuum sector diagrams, *Phys. Lett. B* **797**, 134916 (2019).
  - [58] J. Collins, The non-triviality of the vacuum in light-front quantization: An elementary treatment, arXiv:1801.03960.
  - [59] P. Ullrich and E. Werner, On the problem of mass dependence of the two-point function of the real scalar free massive field on the light cone, *J. Phys. A* **39**, 6057 (2006).
  - [60] F. Coester and W. Polyzou, Vacuum structures in hamiltonian light-front dynamics, *Found. Phys.* **24**, 387 (1994).
  - [61] S. Tsujimaru and K. Yamawaki, Zero mode and symmetry breaking on the light front, *Phys. Rev. D* **57**, 4942 (1998).